

Optimization of the Readout Electronics for Microchannel Plate Delay Line Anodes

John Vallergera and Jason McPhate

Space Science Laboratory, University of California, Berkeley, CA 94720-7450

Many current and future space missions use microchannel plate (MCP) detectors with delay line anode readouts (e.g. FUSE, GALEX and the FUV detector on the upcoming Cosmic Origins Spectrograph (COS) on the Hubble Space Telescope). Delay line anodes are used to measure the position of the centroid of the charge clouds that exit MCP detectors. This is accomplished by measuring the time difference between the arrival of the pulse at both ends of the delay line. The spatial resolution of this position determination is dependent on the accuracy of the temporal measurement. These high frequency pulses (~100MHz) are usually amplified and directed to constant fraction discriminators (CFDs) whose output pulses start and stop a time to amplitude converter (TAC).

This paper reviews the optimization of these circuit elements. It includes the characteristics of various delay line types (serpentine and helical) and their effect on pulse shape. The choice of amplifier filter bandpass and optimum fraction and delay for the CFDs is also presented. Examples are taken from the MCP detectors on the missions mentioned above.

Keywords: Microchannel plates, UV detectors, constant fraction discriminators, delay line anodes.

1. INTRODUCTION

Microchannel plate detectors with delay line anodes as the photon event readout are employed on many current and future space missions such as UVCS and SUMER on SOHO¹, FUSE², Spectrographic Imager on Image³, GALEX⁴, and COS⁵ to be installed on Hubble in 2003. Delay line anodes^{6,7} detect the location of the incident event by the arrival time difference of the MCP output charge pulse at each end of the anode. MCP detectors of this type have been able to achieve spatial resolutions less than 25 μm FWHM⁵ over a dimension of 85 mm and can operate at count rates greater than 100kHz⁸. However, to achieve these results in a single detector requires the careful optimization of the readout electronics used to time the pulses from the anode. This paper will start with a simplified discussion of the readout electronics and how they work and then theoretically derive some optimization parameters for an ideal case. These parameters can then be used as “starting points” for further empirical optimization when confronted with signals from real anodes and electronics for which examples are given from the COS and GALEX detectors.

1.1 Delay Line Anodes

When a charge pulse from an MCP set impinges at a specific position on a delay line anode, the pulse splits in two and travels in both directions along the delay line. The time *difference* between the time of arrival of each pulse at both ends of the anode is linearly proportional to the original position on the anode and inversely proportional to the velocity of propagation of the pulses in that dimension. To minimize the error in the determination of the position (*i.e.* optimize spatial resolution) one must decrease the velocity of propagation as much as possible and minimize the timing error of both pulses. The geometry, layout and materials of the of the delay line determine the velocity of the pulses while the timing error is usually determined by the pulse sensing electronics. The two are not completely independent, however, as certain choices of very slow delay line patterns can adversely affect the pulse shape which in turn increase the timing error. Typical delay line velocities are on the order of 1 mm ns⁻¹ while output pulses are about 5 ns wide. Therefore to achieve a spatial accuracy of 25 μm requires that the measurement of the arrival time of this 5ns pulse be accurate to 25ps.

The Experimental Astrophysics Group at the Space Science Laboratory, University of California, Berkeley, has used an assortment of delay line patterns to collect the MCP charge pulses. “Serpentine” and “Helical” delay lines refer to a single or multi-planar delay line patterns, respectively (Fig 1). When used as actual anodes, they are usually connected to conducting “strips” so that the delay line is separated from the active charge collection region. Examples of this are: the “Double Delay Line or DDL⁷” where the strips are wedges and the orthogonal coordinate is determined by a charge division scheme between the wedges; and the Cross Delay Line or XDL, where two orthogonal sets of fingers cover the active charge collection region and each set is connected to a delay line (of either type). A hybrid scheme (used in COS on Hubble) uses a helical delay line directly to encode one dimension (no strips) while the other dimension uses strips and a small helical delay line. The choice of anode pattern is usually based on size of detector, the resolution requirement in each dimension, and the cost and reliability of the fabrication techniques.

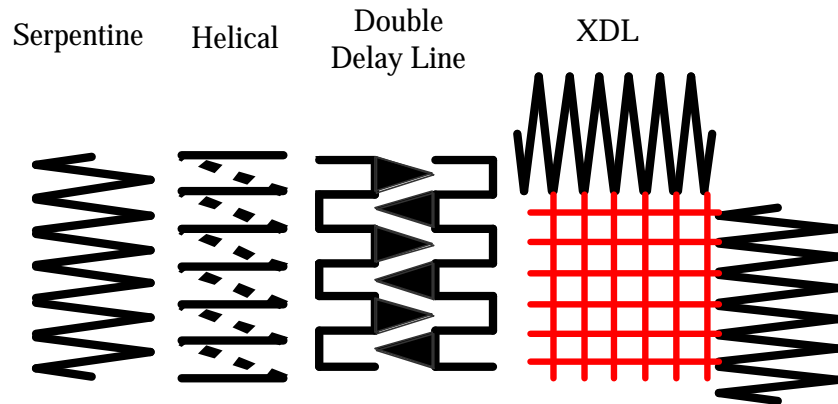


Figure 1. Delay Line nomenclature. The Serpentine is a planar zig-zag pattern while the Helical is multi-planar pattern where the dotted lines represent the opposite side of a 3 level structure. There is a ground plane in between the two levels and the top and bottom patterns are connected by vias. The Double Delay Line (DDL) and Cross Delay Line (XDL) are delay line anode patterns where the charges collected on strips which are tapped into the delay lines, which can be serpentine or helical. The DDL anode uses a charge division scheme to measure the orthogonal axis.

The impact of delay line choice on the timing electronics is the effect that it has on the pulse shape. Both helical and serpentine delay lines are not perfect transmission lines and do not have a linear phase characteristic essential to avoid pulse dispersion, preshoot and ringing. Pulses widen as they traverse the delay line and lose amplitude. Most of this is due to capacitive and inductive coupling along the delay line. When unterminated strips are attached at every bend in the delay line, as in the DDL or XDL anodes, a fraction of each pulse must travel down these strips to be reflected back into the pulse but at a later time dependent on strip length. These strips act as resonance filters and tend to slow the velocity and widen the pulse. Figure 2 shows examples of two different pulse shapes exiting a helical and serpentine delay line.

1.2 Timing Electronics

A simple schematic of the one dimensional delay line readout electronics is shown in Figure 3. Pulses from each side of the anode (~ 10 mV, 5ns wide) are amplified, high and low pass filtered and then sent to a Constant Fraction Discriminator (CFD). The CFDs produce the ECL logic pulses to start and stop a Time to Amplitude Converter (TAC) which outputs an analog voltage pulse whose amplitude is proportional to the time difference of the start and stop signals. This pulse is then digitized and represents the pixel location of the input pulse. Since the delay lines are usually symmetric, the start and stop designations are arbitrary until an extra delay is added on the stop side to ensure that start always comes before stop for a given pulse. The added delay on the stop side can either be before or after the CFD. We usually add the delay after the CFD with a compact lumped-delay circuit. The lumped delay can degrade the pulse shape, however this is not much of a concern for a large ECL pulse. The alternative is to add an extra length of low dispersion cable to the input to the stop CFD, but this is a very bulky implementation when the delays of the anode are on the order of a hundred nanoseconds.

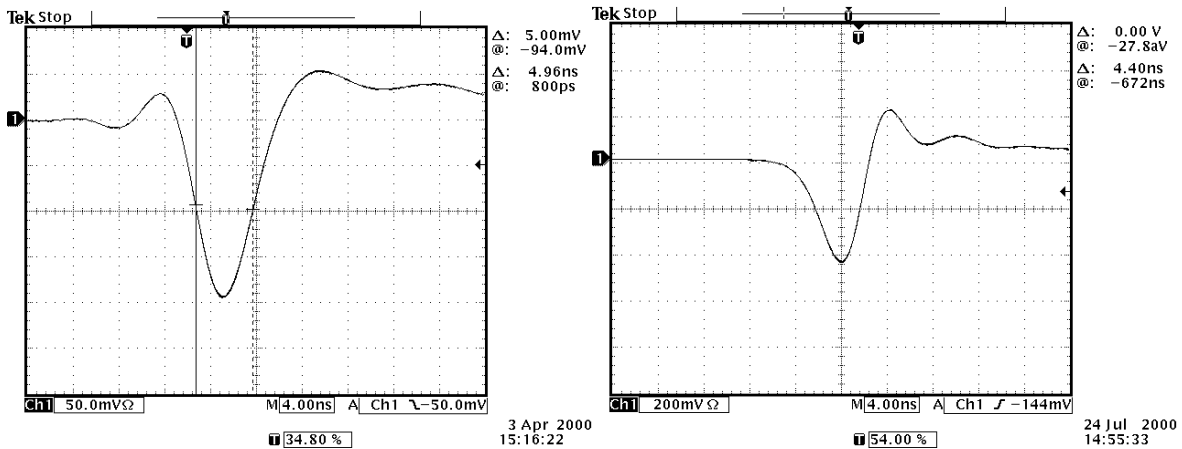


Figure 2. Example pulse shapes. The left oscilloscope trace is an amplified and filtered pulse out of a helical delay line while the right oscilloscope trace is from a serpentine XDL anode. Note the faster leading edge on the helical pulse and the faster trailing edge on the XDL pulse.

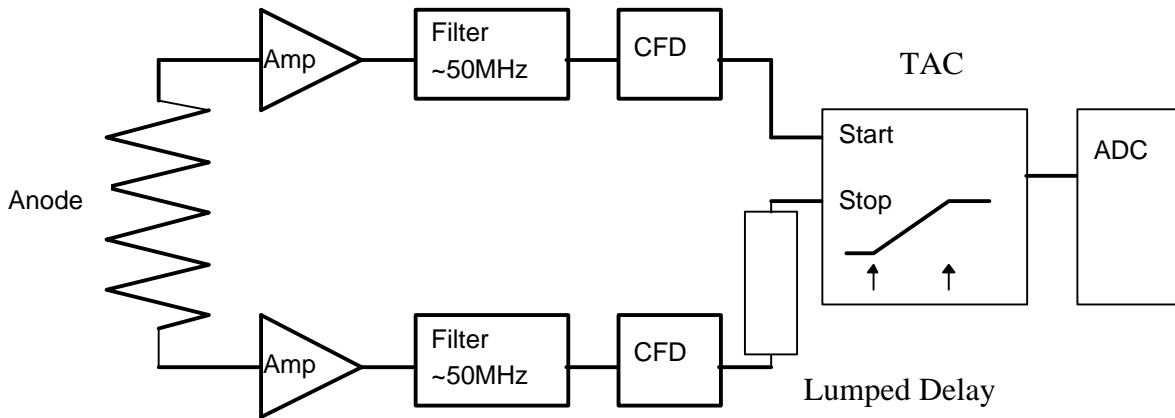


Figure 3. Simple schematic of delay line timing electronics.

1.2.1 Amplifiers and Filters

High bandwidth, low noise amplifiers are necessary for delay line anodes to get the best timing performance. However, filters must be added to optimize the pulse shape for the downstream CFDs (see below). The choice of the filter depends again on the pulse shape. Typically a 100MHz, Chebyshev filter is used for its sharp high frequency cutoff while a simple RC filter is used for the low frequency. The linearity of the amp is also important; not only for the dynamic range of the MCP pulses due to wide pulse height distributions, but also large dispersion in the anode. A factor of 3 in pulse height range and a factor of 2 in amplitude caused by dispersion results in a dynamic range of 6 for which the amplifier must be linear. Amplifier non-linearities can result in amplitude dependent timing errors.

1.2.2 Constant Fraction Discriminators

The heart of the timing circuit is the CFD. Its purpose is to detect an input analog pulse and generate a fast logic pulse with a constant fixed offset in time with respect to the pulse. This temporal offset should not be a function of pulse amplitude (so called “walk”). The CFD does this by subtracting a delayed version of the pulse from a fraction of the pulse (Fig 4), though there are other techniques^{9,10}. When the result of the subtraction crosses zero, the logic pulse is generated (Fig. 5) and the time of the zero crossing is

independent of the pulse amplitude. The choice of the fraction, F , which can be greater or less than 1, and the delay, t_0 , is the main method of optimizing the CFD with respect to the amplified anode pulse.

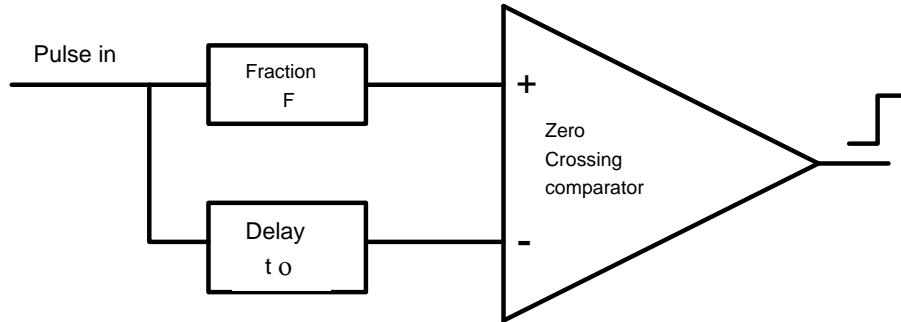


Figure 4. Oversimplified schematic of a CFD. The pulse into the + input of the comparator is multiplied by the fraction F , while the pulse into the - input is delayed by a time t_0 . Not shown is the threshold trigger circuit, the impedance matching, the walk adjustments and the layout details, all of which are important to minimize timing error.

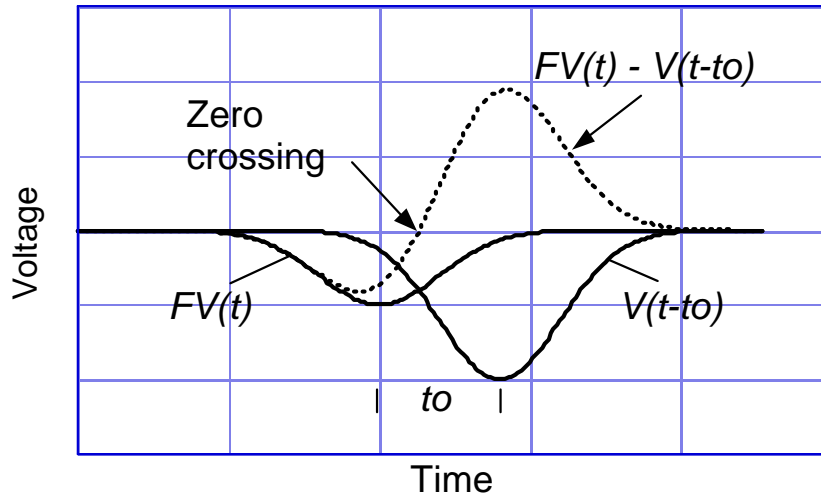


Figure 5. Simulated pulse in circuit of Fig. 4. $V(t)$ is the arbitrary input pulse, F is the fraction and t_0 is the delay. The comparator will trigger when the attenuated input pulse crosses its delayed twin.

1.2.3 Time to Amplitude Converter and ADC

The TAC creates a voltage pulse whose amplitude is proportional to the difference in arrival time between the start and stop pulses. A very simplified description of how this works is by integrating a constant current source on a high quality capacitor where the start and stop pulses start and stop the integration, respectively. Though the TAC and the ADC are key parts of the readout electronics, their optimization is not truly dependent on the delay line or pulse shapes and therefore are outside the scope of this paper and will not be discussed. However, much work has gone into improving the TAC for delay line use. In particular, preserving the timing accuracy as the input pulse rate increases beyond 100kHz⁸.

2. OPTIMIZATION OF THE ELECTRONIC FRONT END

Given an arbitrary pulse shape that comes out of the amplifier, what is the best choice for the delay and fraction of the CFD? This section presents a derivation of the optimum choice of these two parameters assuming the CFD behaves ideally as shown in Figs. 4 and 5 and the pulse is well behaved. These optimum values should be considered as starting points in the empirical search for the true optimum values with real electronics and real pulses; examples of which are shown in the following section.

2.1 Choice of Fraction in “Constant Fraction”

Let $V(t)$ represent the input voltage pulse as an (arbitrary) function of time. Let $G(t)$ be the difference between this pulse, multiplied by the fraction, F , and its delayed image $V(t-t_0)$:

$$G(t) = FV(t) - V(t - t_0) \quad (1)$$

$G(t)$ represents the voltage difference between the two comparator inputs. The zero crossing comparator changes logic state when the function G crosses zero at time T , and it is this digital logic signal which is used downstream in the electronics to time the pulse. This zero crossing time is independent of the amplitude of $V(t)$. However, noise fluctuations of $V(t)$ (and therefore $G(t)$) will cause a corresponding timing noise in the zero crossing time. Let σ_t , σ_G , and σ_V be the error in the zero crossing time, T , the difference signal, $G(t)$, and the voltage pulse, $V(t)$ respectively. Then

$$s_t = \frac{s_G}{dG(t)/dt} \Big|_T \quad (2)$$

where the slope of G is analyzed at T . Assuming the noise variance in $V(t)$ is the same a time t_0 later, though uncorrelated, the variance of G , s_G^2 , is then given by

$$s_G^2 = \left(\frac{\int G}{\int V(t)} \right)^2 s_{V(t)}^2 + \left(\frac{\int G}{\int V(t-t_0)} \right)^2 s_{V(t-t_0)}^2 \quad (3)$$

$$s_G^2 = F^2 s_{V(t)}^2 + s_{V(t-t_0)}^2 (= s_{V(t)}^2) \quad (4)$$

$$s_G = s_{V(t)} (F^2 + 1)^{1/2} \quad (5)$$

The assumption that the voltage noise is uncorrelated over a time, t_0 , is true for the higher frequency noise components which are the dominant contributor. For the lower frequency noise, ($\nu \ll 1/t_0$), the difference circuit effectively removes the noise contribution, acting as a high pass filter. Now substituting this result, along with the following identity, into the equation for σ_t :

$$\frac{dG}{dt} = F \frac{dV(t)}{dt} - \frac{dV(t-t_0)}{dt} \quad (6)$$

$$s_t = \frac{s_{V(t)} (F^2 + 1)^{1/2}}{F \frac{dV(t)}{dt} - \frac{dV(t-t_0)}{dt}} \quad (7)$$

We want to optimize the choice of the constant fraction, F , to minimize the error in the time determination, σ_t . We therefore differentiate σ_t with respect to F and set it equal to zero.

$$\frac{ds_t}{dF} = 0 \quad (8)$$

$$F \left(\frac{dV(t)}{dt} - \frac{dV(t-t_0)}{dt} \right) = (F^2 + 1) \frac{dV(t)}{dt} \quad (9)$$

$$F = - \left(\frac{\frac{dV(t)}{dt}}{\frac{dV(t-t_0)}{dt}} \right) \quad (10)$$

This equation must be analyzed at the crossing time, T . $dV(T)/dt$ is just the slope of the trailing edge of the unattenuated prompt pulse while $dV(T-t_0)/dt$ is the slope of the leading edge of the delayed pulse, both analyzed at the crossing time. The equation simply states that the optimum fraction for an arbitrary

pulse shape is the ratio of the slopes at the zero crossing time. The fraction can be either greater or less than 1.0. The optimum fraction for a symmetric pulse (e.g. gaussian shape) is 1.0. Controlling the fraction value allows one to weight the edge with the greater signal to noise ratio, where the signal in this case is a steep slope.

2.2 Choice of Delay

The choice of CFD delay is usually done first, before the fraction, since to determine the optimum fraction the crossing point must be known. We are discussing this parameter second to use the equations already derived. Using the equation for σ_t above, the optimum delay, t_0 , is derived by differentiating the equation with respect to t_0 . However, t_0 is embedded in the pulse shape $V(t-t_0)$, which has been arbitrary up to this point. The choice of the optimum delay is therefore dependent on the exact pulse shape. A simple example is a triangular shaped pulse. The numerator and denominator of equation (10) stay fixed for a wide range of t_0 , where the leading and trailing edges cross, and all these choices of t_0 are optimum.

A more illustrative example would be a symmetric, gaussian shaped pulse:

$$V(t) = \exp\left(-t^2 / 2\mathbf{S}^2\right) \quad (11)$$

Differentiating σ_t with respect to t_0 and setting the result to zero, produces:

$$\frac{d}{dt_0} \left(F \frac{dV(t)}{dt} - \frac{dV(t-t_0)}{dt} \right) = 0 \quad (12)$$

$$\frac{d}{dt_0} \left(\frac{-(t-t_0)}{\mathbf{S}^2} \exp\left(\frac{-(t-t_0)^2}{2\mathbf{S}^2}\right) \right) = 0 \quad (13)$$

$$\mathbf{S}^2 = (t-t_0)^2 \quad (14)$$

This last equation must be analyzed at the zero crossing time, T. In this example of a symmetric pulse shape, the crossing time is just $t_0/2$ so substituting this for t gives the optimum delay for a symmetric, gaussian shape:

$$t_0 = 2\mathbf{S} \quad (15)$$

This delay is slightly shorter than the FWHM of a gaussian pulse ($= 2.355\sigma$) and corresponds to having the pulse cross itself at its inflection points where the slope is greatest. This then confirms the common sense approach to choosing a delay for any shape pulse by having the steepest parts of the leading and trailing edges cross.

3. REAL SIGNAL COMPLICATIONS

3.1 Dispersion and Pulse Shape

As mentioned above, the helical and serpentine delay lines suffer from dispersion. Dispersion makes the optimization of the CFDs difficult since one single pulse shape can't be assumed. Not only do the pulses get wider with dispersion, but also the ratio of the slopes of the leading and trailing edges change. Figure 6 is an oscilloscope trace of both the start and stop pulses (amplified) from the helical cross delay line of COS (the long helical dimension without the fingers). In this case the event was located near the start side, so the start pulse leaves the anode quickly without traversing much of the delay line. The pulse is clean and narrow. The stop pulse appears ~70 ns later, wider and with less amplitude and with a leading precursor wiggle.

If the delay and fraction for the CFD is chosen based on the average pulse from the anode, the resolution would be best at the center of the anode and would degrade towards the ends, since both the prompt pulse would be narrower and the delayed pulse would be wider. We combat this effect by bandpass filtering the pulses to make the pulses from throughout the anode appear more uniform. This can slightly degrade the best performance in the anode middle, but greatly improve the resolution at the ends

The particular example of Fig. 6 uses both a low pass filter to decrease the amplitude of the leading precursors so as to not start false triggers of the CFD as well as a high pass filter to remove the lower frequency pulse tails (hence the bipolar nature of the pulses). Again, optimum choice of the exact filter values depends on the shape of the raw anode pulse. Smaller anodes can have very good dispersive qualities and the filtering can be minimal with fraction and delay given by the equations above. The large anodes used by COS, GALEX, and FUSE required an intensive empirical optimization effort to match the anode characteristics with the electronics using the filters and CFD settings.

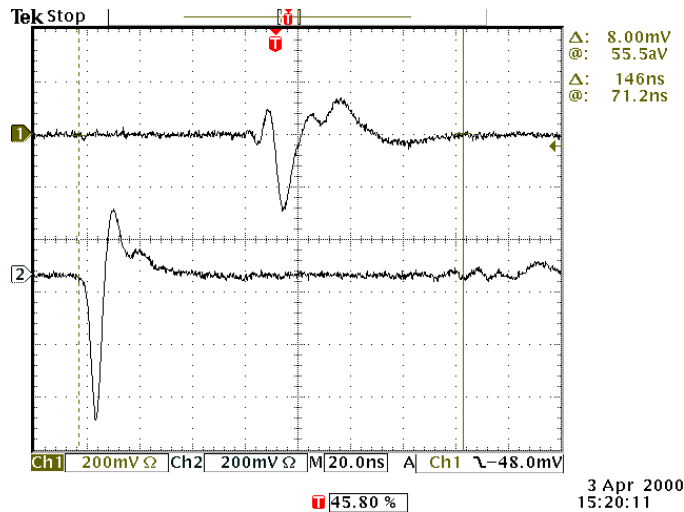


Figure 6. Anode dispersion. Oscilloscope trace of both start (bottom) and stop (top) outputs from a single event near the start side of the anode. The prompt pulse leaves the anode mostly unaffected while the delayed pulse shows the effects of dispersion: increased width and decreased amplitude. Note the reflection of the stop signal appearing on the start trace 140-180 ns after the start signal has left the anode.

3.2 Reflections and Baseline Disturbance

Every attempt is made in designing the anode pattern to keep the delay line transmission line characteristic impedance at 50 . However, given the tolerances of the various dielectric layers and line widths, it is rare to match 50 exactly. When coupling to a 50 feedthrough and cable, reflections of the pulses occur which can disrupt the baseline. This normally would not be a problem, as a reflection from a start pulse leaving the anode would not catch up with the stop pulse going the other way. Unfortunately, given the dispersion of the helical anodes, higher frequency components of the reflection can race ahead (at low amplitude) and get to the anode output before the real pulse. This disturbance is too small to trigger the CFDs but it does disrupt the baseline and can affect the pulse shape of the real pulse and therefore the position of the event. The signature of this effect is a non-linearity in the measured position vs. the true position and can be observed in a modulation of the detector flat field as well as resolution mask patterns. The velocity differences are slight enough that this is only a problem for long anodes and events that occur near the ends. Fig. 6 shows a baseline disturbance due to the reflection of the start signal. To ameliorate this effect requires a better impedance match, less dispersion, or separating the active area of the anode away from the reflective interfaces by increasing the total anode length or decreasing its active field of view.

3.3 Amplifier Non-Linearity

Another real world effect that can degrade resolution for a delay line detector are amplifier non-linearities. If the amplifier is non-linear, the pulse shape will be different for pulses with the same shape but different amplitudes. This will result in different zero crossing times in the CFDs for different amplitudes. Figure 7 is an oscilloscope trace of two pulses from the same amplifier, with the input amplitude different by 10db. (To keep the signals in the same range for the oscilloscope, the same 10 dB attenuator was move from the input to the output of the amplifier). This effect is not seen in the center of the anode because the shift in time would be the same for both start and stop since they would be of the same amplitude and therefore the shift would subtract out using start - stop. But at the ends of the anode, where the dispersion effect is greatest, a single event would have the start amplitude appreciably different than the stop amplitude and the resultant position determined would depend on amplitude, especially at the higher pulse heights where the amplifier non-linearities are at their worst. Again, to defeat this effect, use low dispersion anodes, operate in the linear regime of the fast amplifiers and use MCPs with narrow pulse height distributions,

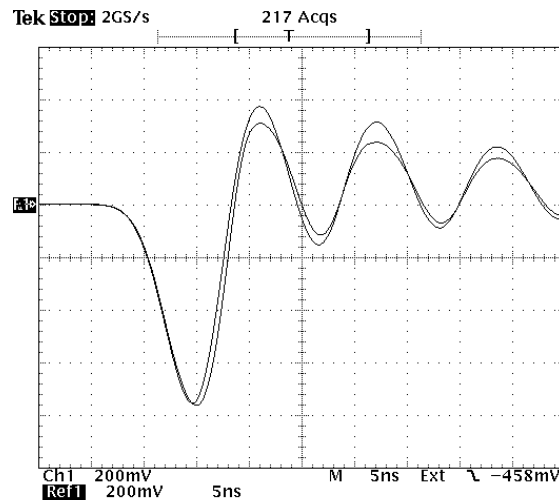


Figure 7. Oscilloscope traces of two pulses out of a fast amplifier. In one case a 10 dB attenuator was placed on the input of the amp while in the second case the same attenuator was placed on the output of the amp. The amplifier in this case is being overdriven and has a non-linear response which results in a different zero crossing.

ACKNOWLEDGEMENTS

This work was supported by NASA under contract NAS 5-98043

REFERENCES

1. Siegmund, Oswald H.; Stock, Joseph M., Marsh, Daniel R.; Gummin, Mark A., Raffanti, Richard; Hull, Jeffrey; Gaines, Geoffrey A.; Welsh, Barry Y., Donakowski, B.; Jelinsky, Patrick N., Sasseen, Timothy; Tom, James L., Higgins, B.; Magoncelli, T., Hamilton, Jon W.; Battel, Steven J., Poland, Arthur I.; Jhabvala, Murzy D., Sizemore, K.; Shannon, J., "Delay Line Detectors for the UVCS and SUMER Instruments on the SOHO Satellite", *Proc. SPIE*, **2280**, pp. 89-100 (1994)
2. Siegmund, Oswald H.; Gummin, Mark A., Stock, Joseph M.; Naletto, Giampiero, Gaines, Geoffrey A.; Raffanti, Richard, Hull, Jeffrey; Abiad, Robert Rodriguez-Bell, Ted; Magoncelli, Tony; Jelinsky, Patrick N. Donakowski, William, Kromer, Karl E. "Performance of the double delay line microchannel plate detectors for the Far Ultraviolet Spectroscopic Explorer", *Proc. SPIE*, **3114**, pp. 283 (1997).
3. Stock, Joseph M.; Siegmund, Oswald H.; Hull, Jeffrey S.; Kromer, Karl E.; Jelinsky, Sharon R.; Heeterks, H. D. Lampton, Michael L.; Mende, Stephen B., "Cross-delay-line microchannel plate detectors for the Spectrographic Imager on the IMAGE satellite" *Proc. SPIE*, **3445**, 407, (1998)

4. Siegmund, Oswald H.; Jelinsky, Patrick N.; Jelinsky, Sharon R. Stock, Joseph M., Hull, Jeffrey S. Doliber, Darrel L., Zaninovich, Jure, Tremsin, Anton S., Kromer, Karl E. "High-resolution cross delay line detectors for *Proc. SPIE*, **3765**,. 429 (1999)
5. McPhate, J., Siegmund, O., Gaines, G. Vallerger, J., and Hull, J., "The Cosmic Origins Spectrograph FUV Detector, *Proc. SPIE*, **4139** (2000) (this conference).
6. Lampton, M. O.H.W. Siegmund, and R. Raffanti, *Review of Scientific Instruments*, **58(12)**, 2299 - 2307 (1987).
7. Siegmund, O.H.W., Raffanti, R., Lampton, M., Herrick, W. and Stock, J., "High resolution delay line readouts for microchannel plates", *Nucl. Inst. Meth.* **A310**, 311-316 (1991).
8. Vallerger, J. "2K x 2K resolution element photon counting MCP sensor with > 200 kHz event rate *Nucl. Instr. Meth. in Phy. Res. A*, **442**, 159, (2000).
9. Turko, B. T. and R. C. Smith,. *IEEE Trans. Nucl. Sci.* NS-38, 711, (1991)
10. Lampton, M. "A timing discriminator for space flight applications", *Rev Sci. Instrum*, **69**, 3062, (1998)